Evaluating the MJO Forecast Skill from Different Configurations of NCEP GEFS Extended Forecast

Wei Li*[2], Yuejian Zhu[1], Xiaqiong Zhou[2], Dingchen Hou[1], Eric Sinsky[2]

Christopher Melhauser[2], Malaquias Peña[3], Hong Guan[4], Richard Wobus[2]

[1]EMC, NCEP, NWS, NOAA, College Park, MD 20740

[2]IMSG at EMC, NCEP, NWS, NOAA, College Park, MD 20740

[3]University of Connecticut, Storrs, CT 06269

[4]SRG at EMC, NCEP, NWS, NOAA, College Park, MD 20740

DRAFT

Journal of Climate

Submitted December 15, 2017

* Corresponding author address: Wei Li, IMSG at Environmental Modeling Center/NCEP/NOAA, 5830 University Research Court, College Park, MD 20740. Wei.Li@noaa.gov

Abstract

NOAA is accelerating its efforts to improve the numerical guidance and prediction capability for extended range (weeks 3 & 4) prediction in its seamless forecast system. Madden Julian Oscillation (MJO) is the dominant mode of sub-seasonal variability in tropics and forecast skill of MJO is investigated in this paper.

We used different configurations of the NCEP Global Ensemble Forecast System (GEFS) to perform the experiments. The configurations include: (1) The operational version of the stochastic perturbation forced with operational Sea Surface Temperatures (SSTs); (2) An updated stochastic physics forced with operational SSTs; (3) An updated stochastic physics forced with bias-corrected SSTs that are from Climate Forecast System (Version 2); and (4) As in (3) but with the addition of a scale aware-convection scheme.

We evaluated MJO forecast skill from the experiments using Wheeler-Hendon indices and also examined the performance of the forecast system on prediction of key MJO components. We found that using the updated stochastic scheme improved the MJO prediction lead-time by about 4 days. Further updating the underlying SSTs with the bias corrected CFSv2 forecast increased the MJO prediction lead time by another 1.7 days. The best configuration of the four experiments is the last configuration which extends forecast lead time by ~9 days. Further investigation shows that upper and

DRAFT

lower level zonal wind has larger contribution to the improvement of the MJO prediction than the outgoing longwave radiation. The improvement of the MJO forecast skill appears to be due primarily to the improvement in the representation of convection and associated circulations over the tropical West Pacific.

DRAFT

1. Introduction

A skillful forecast for the sub-seasonal time scale (3-4 weeks) is valuable in socio-economic context but poses substantial challenges. The limited forecast skill for this time window is mainly due to its relatively weak dependence on the initial conditions (an important source of predictability for the short term weather forecasts) and the insufficient time for the forecast system to 'feel' the effects of the lower boundary forcing that provide predictability on seasonal and longer timescales (Vitart et al., 2009, Johnson et al. 2014; Liu et al. 2016, Troccoli 2010, Tian et al. 2017). Thus improving sub-seasonal forecasts is likely to come from substantial efforts on the model development, with a focus on improving representation of the sources of the sub-seasonal predictability.

As a dominant mode in tropical variability on the sub-seasonal timescale, the Madden-Julian Oscillation (MJO), which features as a 30-60 day oscillation of convection and precipitation in the tropics has been a focal point of the research community and operational centers that are looking to improve sub-seasonal prediction. Indeed, numerical studies have found that improvement in tropical and extratropical prediction on sub-seasonal time scale can be linked to improved prediction of the MJO (Ferranti et al., 1990; Waliser et al. 2003; Lin and Brunet 2009, Pegion and Sardeshmukh 2011; Vitart 2014; Liu et al. 2017). With increasing interest and demand for skillful sub-seasonal forecasts, better representation of the MJO is of particular importance in operational Numerical Weather Prediction (NWP) centers. In recent years, progress in MJO forecasting as a result of NWP developments has been quite promising. For

DRAFT

example, the European Centre for Medium-Range Weather Forecasts (ECMWF) has mitigated the temporal decline in MJO prediction skill by about 1 day per year since 2002 (Vitart 2014). It was found that the large improvement before 2009 was mostly attributed to the change in convective parameterization (Vitart 2009). The progress of MJO forecast skill offers promise for corresponding potential improvements in the sub-seasonal forecast for most of other phenomena.

Concerning the MJO prediction/forecast, researchers and model developers mainly focus on these key areas for skill improvement and they are: 1). model physics parameterization: particularly, the MJO skill was found to be sensitive to the convection scheme and some research suggested the improvement of the skill through the MJO propagation (Wang and Schlesinger 1999; Maloney and Hartmann 2001; Liu et al. 2005; Lin et al. 2008; Zhang and Song 2009; Vitart 2009; Zhou et al. 2012). 2). Ocean impact. The MJO is mainly an atmospheric phenomenon but ocean impacts, particularly the accurate sea surface temperatures and atmospheric ocean coupling are believed to be critically important for prediction (Wang et al. 2015; Liu et al. 2017). 3). Ensemble prediction using either single model (Vitart and Molteni 2010; Hudson et al. 2013) or multi-model approaches to effectively sample model uncertainty (Gottschalck et al. 2010; Fu et al. 2013). The National Center for Environmental Prediction (NCEP) Global ensemble Forecast System (GEFS) provides numerical guidance for probabilistic forecast with the lead time up to 16 days. To align with the NOAA effort to accelerate sub-seasonal prediction in a seamless ensemble forecast system, several experiments that extend the GEFS integration time to cover weeks 3 & 4 lead time were performed. Using this approach, an early investigation indicated that MJO prediction skill was improved by using an optimal SST

DRAFT

scheme (Zhu et al. 2017a). Following that investigation, we have performed more comprehensive experiments to test the impact of using different GEFS configurations on MJO forecast skill.

The results of some of these experiments are described herein., specifically, this study focuses on three scientific areas: 1). A new perturbed physics scheme designed to sample the model uncertainty more effectively over the tropical region; 2). An updated underlying SST that represents the day-to-day variability from a coupled atmosphere-ocean model; and 3). An updated scale dependent convection scheme and other changes to the physics parameterizations (Han et al. 2017). For these experiments, the focus is on a 2-year period with new forecasts launched every 5 days. This approach allows us to sample the MJO phenomenon sufficiently while keeping computational expense manageable.

Section 2 describes the details of the experiments and data used in this study. The evaluation of the forecast skill of the MJO and its associated key components is demonstrated in section 3. Conclusions and discussion are provided in section 4.

2. Experiment and Data

The NCEP Global Ensemble Forecast System (GEFS version 11, Zhou et. al, 2017), based on the Global Forecast System version 12 (GFS, i.e. Global spectral model GSM + land surface model LSM) is used to perform the experiments. For each experiment, a 21- member (1 control

run and 20 perturbed members) ensemble was used to integrate the forecast system that run up to 35 days. Considering the computational cost and the relatively small impact of the resolution on longer lead times (Tracton and Kalnay 1993; Ma et al. 2012), we used relatively coarse T574 horizontal resolution (roughly equivalent to 33km grid spacing) for the first 8 lead days and T382 (~55km) for lead days 8-35. 64 vertical levels were used for all lead times. Because GFS is an uncoupled atmosphere ocean forecast system, a prescribed SST with the initial analysis data damping towards the observed climatology (with a 90-day e-folding rate) was used to force the model. The Simplified Arakawa-Schubert convective parameterization scheme was used for deep convection (SAS, Arakawa and Schubert 1974; Grell 1993; Pan and Wu 1995; Han and Pan 2011) and the Mass-flux shallow convection scheme for shallow convection. Documentation of the GFS operational Physics can be found in (http://www.dtcenter.org/GMTB/gfs_phys_doc/).

In this study, four experiments were conducted to examine the MJO forecast associated with different GEFS configurations. The four configurations were: 1). an operational version of the GEFS that uses the Stochastic Total Tendency Perturbation scheme (Hou et al. 2006, 2008) and that is extended to 35 days without changing the SSTs (hereafter STTP); 2) same as 1) but using an updated stochastic physics scheme that combines Stochastic Perturbed Physics Tendency (SPPT, Buizza et al 1999; Palmer et al, 2009), Stochastic Humidity Perturbation (SHUM, Tompkins and Berner 2008) , and Stochastic Kinetic Energy Backscatter (SKEB) (Shutts and Palmer, 2004; Shutts 2005; Berner et al. 2009 hereafter SPs); 3). same as 2) but forced with bias corrected CFSv2 forecast SST (hereafter SPs+CFSBC); and 4). same as 3) but using a scale aware-convection scheme (SPs+CFSBC+CNV) in GSM (Han et al. 2017). Table 1 summarized

DRAFT

the configurations of all these experiments. All experiments were initialized every 5 days at 00Z, starting May 1st 2014 and ending May 26, 2016.

The analysis data used in this study is the NCEP GFS analysis, i.e., Global Data Assimilation System (GDAS). A 7-point daily mean centered at 00Z of each lead day (e.g. using 06Z, 12Z, 18Z 24Z, 30Z, 36Z and 42Z average to represent the daily mean of the lead day 1) is used in both forecast and analysis data. Both forecast and analysis data are at 2.5 degree resolution.

3. Results

3.1. MJO forecast skill

We evaluated the Wheeler Hendon (WH) MJO indices (Wheeler and Hendon 2004), which is defined as the bivariate anomaly correlation between the analysis and forecast Realtime Multivariate MJO (RMM1) and (RMM2) using input fields of outgoing longwave radiation (OLR), zonal wind at 200 hPa and 850 hPa. i.e.

$$AC(\tau) = \frac{\sum_{i=1}^{N}[a_1(t)f_1(t,\tau) + a_2(t)f_2(t,\tau)]}{\sqrt{\sum_{i=1}^{N}[a_1^2(t) + a_2^2(t)]}\sqrt{\sum_{i=1}^{N}[f_1^2(t,\tau) + f_2^2(t,\tau)]}} \quad (1)$$

DRAFT

where f_1(t, τ) and f_2(t, τ) are the RMM1 and RMM2 of the forecast at lead day τ initialized at day t. $a_1(t)$and $a_2(t)$ are the RMM1 and RMM2 of the analysis data corresponding to the forecast at day t.

The MJO forecast skill of the GEFS with the updated stochastic physics schemes, SST scheme and convection scheme showed improvement from the operational GEFS with each successive enhancement (Fig. 1). By only changing the stochastic schemes, the MJO forecast skill improved from ~12.5 days (defined as anomaly correlation equals to 0.5) to ~ 16.8 days. Further updating the underlying SST improved the MJO forecast skill by another 1.7 days and updating all three areas of the GEFS (configuration 4) improved the MJO skill to 22 days (Figure 1a). In the GEFS forecast, the skill of RMM2 is greater than RMM1 (cf. Figs. 1b and 1c), leaving an open question whether the forecast over the Maritime continent and tropical Africa is more skillful than that over tropical West Pacific and Indian Ocean.

The forecast MJO strength varies with initial time (Fig. 2). The MJO strength associated with SPs, SPs+CFSBC and SPs+CFSBC+CNV are similar while the MJO strength from the STTP experiment is generally stronger than the strength in other three experiments. For both lead days 16 and 21 (Fig. 2ab), the forecast MJO is not systematically stronger or weaker than the analysis in each experiment, indicating the forecast MJO strength is dependent on initial time. For the periods of July to November of 2015 and February to March of 2016, the forecast MJO strength is more consistent with the analysis than it is for the other initial periods of the two years for both lead days (Fig. 2ab).

DRAFT

The progression of the MJO in different phases is also dependent on initial time. For the two example initial periods, in April-October 2015 (validation time for lead day 16 is May-October 2015, Fig.3ab), the forecast MJO indices are weaker in the SPs, SPs+CFSBC and SPs+CFSBC+CNV experiments than in the STTP experiment. The strength of the MJO in the SPs+CFSBC+CNV experiment is more similar to that in the analysis than in the MJO in the other experiments but still much weaker than the analyzed MJO. In the initial period of September-December 2015 (Fig.3cd), the forecast MJO strength is closer to the analysis data in all experiments but there are phase errors. For both initial periods, the SPs experiments perform better than the STTP. For all experiments, the forecast MJO tends to shift to the left side of the phase diagram, i.e. Western Hemisphere, Africa and Indian Ocean which suggests that the forecast MJO fails to propagate appropriately over the West Pacific ocean and Maritime Continent. Thus, there are deficiencies in both magnitude and sign of the forecast RMM1 and RMM2 in the forecast system for the weeks 3 & 4 time scale.

3.2. Contribution of the large-scale circulation and convection

Since the Wheeler-Hendon MJO skill uses the upper and lower level zonal wind and the OLR anomaly to represent MJO associated circulation, the forecast skill of the large-scale circulation and the convection are examined to help better understand the improvement in MJO skill. Fig. 4 shows the correlation of the tropical 15°S-15°N mean zonal wind and OLR anomaly during the 2-year period (150 initial days) for all lead days and four experiments. In all experiments, the

correlation score for upper level zonal wind is higher than the lower level zonal wind which is higher than the OLR. This is reasonable because lower level winds are more dependent on the model uncertainty in surface process than are the upper level winds. The OLR forecast shows the lowest score, likely because it is a function of more complicated physical and dynamical processes that involves considerable uncertainty thus limiting the forecast skill. For all three components, it is obvious that all the SPs experiments (including SPs, SPs+CFSBC and SPs+CFSBC+CNV) performed better than the production version of the GEFS (STTP), indicating the positive impact of these updated stochastic scheme on the performance of the forecast system over the tropical region. Among the SPs experiments, SPs+CFSBC+CNV outperformed SPs+CFSBC which outperformed SPs in wind components, especially in 200 hPa zonal wind. Although there are some differences between the SPs and the other two experiments (i.e. SPs+CFSBC and SPs+CFSBC+CNV) in OLR for longer lead time, the difference between the SPs+CFSBC and SPs+CFSBC+CNV is not as evident as in the zonal wind fields.

To further explore where in the tropics does the substantial improvement occur, we examined correlation of the wind and OLR anomaly on each model grid over the tropics for lead day 15 (Fig. 5). The operational version of GEFS shows better performance on 850 hPa zonal wind anomaly forecast than the other two variables over the region from tropical Indian Ocean to west Pacific (Fig. 5 a-c). The updated stochastic schemes that perturbed the temperature, wind and humidity profile help improved the 200 hPa zonal wind anomaly over the tropical Indian Ocean to most of the Maritime Continent, as well as the 850 hPa zonal wind anomaly over the tropical west Pacific and Indian Ocean (Fig. 5 d-f). In the Wheeler-Hendon RMM calculation, the zonal

DRAFT

wind is weighted more than the OLR anomaly. Although the updated stochastic schemes also resulted in an improvement of the OLR anomaly forecast over the MJO related region, the improvement in the wind component appears to be the main reason that leads to the improved MJO forecast in the updated stochastic schemes. A further update on underlying SST, combined with the updated stochastic schemes enhanced the improvement of the three variables. Updated the stochastic scheme, the underlying SST, and the convection scheme provided additional skill to the wind and OLR forecast (Figure5, i-l). The improvement of the forecast anomaly of the three variables can also be demonstrated in a latitude and lead time cross-section of the three variables (Fig. 6). The SPs+CFSBC+CNV is the configuration that leads to the largest improvement. Among the three variables, the largest improvement occurs in 200 hPa zonal wind, especially beyond two weeks of the lead time. The conclusion that of these tested here, the SPs+CFSBC+CNV is the best configuration for MJO forecasts can also be substantiated by a MJO phase and lead time cross-section of the pattern correlation of the composite 200 hPa, 850 hPa zonal wind and OLR fields (Fig. 7). For all three variables, the large improvement occurs mostly on phase 3 and phase 6-7 after two weeks of the lead time. This is consistent with the improvement of the forecast over tropical west Pacific and Indian Ocean (Fig. 5).

3.3. Contribution of the stochastic physics scheme

Based on the evaluation of the forecast skill of the MJO and its associated variables (Fig.1 and 4), the forecast skill exhibits a jump after using an updated stochastic scheme. As such, we examined the spread of the perturbed variables in the SPs experiment to further check the

DRAFT

contribution of the stochastic scheme on the performance of the GEFS. The SPs is a combined stochastic physics scheme of three components, which include SPPT, SHUM and SKEB. The individual impact of the SPs has been discussed in Zhu et al. 2017a. The combined effect of the SPs, compared to the operational STTP version, increased the spread mainly over the tropical region (Fig.8) and the increase of the spread lead to an improved temperature, zonal wind and relative humidity profile in the same region (Fig.9). For the weeks 3 & 4 forecast of the tropical mean zonal wind at 250 hPa and 850 hPa, the forecast skill improved by 43% and 19% respectively (Fig.10). The weeks 3 & 4 forecast skill of the tropical zonal wind is strongly dependent on the initial time. The skill range can be as large as 1 for the zonal wind at both levels. The forecast skill of the weeks 3&4 tropical mean zonal wind at 250 hPa and 850 hPa during a strong MJO period is 63% and 18% larger than that of the weak MJO period in SPs experiment and 50% and 12% larger in STTP experiment. The conclusion that higher skill of the weeks 3&4 forecast is associated with strong MJO period is consistent with the result in figure 2.

4. Conclusion and Discussion

Improving forecast skill for the source of the sub-seasonal predictability (i.e, the MJO) is critical to the improvement of tropical and extratropical forecasts of other phenomena, especially for extreme events. In this work, experiments were performed using different configurations of the NCEP GEFS to evaluate the MJO forecast skill and its key components. Based on the four experiments, it was determined that the MJO forecast benefited largely from the use of a stochastic physics scheme that resulted in the improvement of the forecast of key MJO

DRAFT

component variables. The improvement was mostly attributed to the increase of the spread of the temperature, wind and humidity profiles over the tropics. The addition of an updated underlying SST from the bias corrected CFSv2 forecast and a new convection scheme simulates tropical convective systems more realistically further enhanced the improvement. The improvement of the MJO forecast skill is mainly due to better representation of the circulation and convection over the tropical West Pacific and Indian Ocean, especially in the configuration of SPs+CFSBC+CNV. A combination of the updated stochastic physics perturbation, more realistic SST, and convection scheme in the forecast model led to about a 9-day extension of given skill threshold for MJO forecasts.

Following this work, our next step will be the evaluation for the MJO-skill impacts after bias-correction. Application of this convection is enabled by the recent completion and post processing of an 18-year reforecast. In addition to the evaluation of tropical forecasts, an analysis of the teleconnection relation between tropical and extratropical prediction skill is necessary and critical. The current investigation suggests that there is a statistically significant lag correlation between the North Atlantic Oscillation (NAO) and MJO indices, which encourages further analysis on this direction. The extreme events associated with the MJO and other sources of predictability for sub-seasonal time scale are also included in plans for future studies.

Linking the forecast skill to the configuration of the forecast system, model developers and researchers may also be interested in isolating the impact of the stochastic scheme, the underlying SST, and the convection scheme. Due to the computational cost, the more granular

DRAFT

sensitivity tests were not conducted as part of this work. Rather, the design of each configuration used herein was based on the positive impact of each factor (SPs, SST and convection) derived from small sample tests and early investigation (Zhu et al. 2017b). A more comprehensive investigation s can be left to other researchers who have interest.

Acknowledgement

The authors would like to thank Drs. Walter Kolczynski and Bing Fu for their help on stochastic physics perturbation settings. The authors are grateful to Dr. Xingren Wu on SST experiment discussion. We thank Drs. Qin Zhang, Shuguang Wang, Ping Liu and Wanqiu Wang for providing valuable discussion on MJO. This study is partially supported through NWS OSTI and NOAA's Climate Program Office (CPO)'s Modeling, Analysis, Predictions, and Projections (MAPP) program.

References

Arakawa A. and W.H. Schubert, 1974: Interaction of a cumulus cloud ensemble with the large-scale environment, uppercase Part uppercase I. *Journal of the Atmospheric Sciences*, 31:674–701.

Berner, J., G. J. Shutts, M. Leutbecher, and T. N. Palmer, 2009: A spectral stochastic kinetic

energy backscatter scheme and its impact on flow-dependent predictability in the ECMWF ensemble prediction system, J. Atmos. Sci., 66 (3), 603 – 626,

Buizza, R., M. Milleer, and T. Palmer. 1999: Stochastic representation of model uncertainties in 504 the ECMWF ensemble prediction system, Q. J. R. Meteorol. Soc., 125 (560), 2887 - 2908

Ferranti, L., T. N. Palmer, F. Molteni, and K. Klinker, 1990: Tropical-extratropical interaction associated with the 30–60 day oscillation and its impact on medium and extended range prediction. *J. Atmos. Sci.*, 47, 2177–2199.

Fu, X., J.-Y. Lee, P.-C. Hsu, H. Taniguchi, B. Wang, W. Wang, and S. Weaver, 2013: Multi-model MJO forecasting during DYNAMO/CINDY period. Climate Dyn., 41, 1067–1081, doi:https://doi.org/10.1007/s00382-013-1859-9.

Gottschalck, J., and Coauthors, 2010: A framework for assessing operational Madden–Julian oscillation forecasts: A CLIVAR MJO working group project. *Bull. Amer. Meteor. Soc.*, 91, 1247–1258, doi:10.1175/2010BAMS2816.1.

Grell, Georg, 1993: Prognostic evaluation of assumptions used by cumulus parameterizations. *Monthly Weather Review*, 121(3):764–787, 2016/03/25.

DRAFT

Han, Jongil and H.-L. Pan, 2011: Revision of convection and vertical diffusion schemes in the ncep global forecast system. *Weather and Forecasting*, 26(4):520–533, 2016/03/25.

Han, J., W. Wang, Y. Kwon, S. Hong, V. Tallapragada, and F. Yang, 2017: Updates in the NCEP GFS Cumulus Convection Schemes with Scale and Aerosol Awareness. *Wea. Forecasting*, **32**, 2005–2017.

Hou, D., Z. Toth, and Y. Zhu, 2006: A stochastic parameterization scheme within NCEP Global Ensemble Forecast System. Preprints, *18th Conf. on Probability and Statistics*, Atlanta, GA, Amer. Meteor. Soc., 4.5.

Hou, D., Z. Toth, Y. Zhu, and W. Yang, 2008: Impact of a stochastic perturbation scheme on NCEP Global Ensemble Forecast System. Preprints, *19th Conf. on Probability and Statistics*, New Orleans, LA, Amer. Meteor. Soc., 1.1.

Hudson, D., A. G. Marshall, Y. Yin, O. Alves, and H. Hendon, 2013: Improving intraseasonal prediction with a new ensemble generation strategy. *Mon. Wea. Rev*., 141, 4429–4449, doi:https://doi.org/10.1175/MWR-D-13-00059.1

Johnson, N.C, D. Collins, S. Feldstein, M. L'Heureux, E. Riddle, 2014: Skillful wintertime North American temperature forecasts out to 4 weeks based on the state of ENSO and the MJO. Weather Forecast 29:23–38. doi:10.1175/WAF-D-13-00102.1

DRAFT

Liu, and coauthors, 2017: MJO prediction using the sub-seasonal to seasonal forecast model of Beijing Climate Center, *Climate Dynamics*, 48, 3283-3307.

Lin, H., and G. Brunet, 2009: The influence of the Madden–Julian oscillation on Canadian wintertime surface air temperature. *Mon. Wea. Rev.*, 137, 2250–2262.

Lin, J. L., M. I. Lee, D. Kim, I. S. Kang, and D. M. W. Frierson, 2008: The impacts of convective parameterization and moisture triggering on AGCM-simulated convectively coupled equatorial waves. *J. Climate*, 21, 883–909.

Liu, P., B. Wang, K.R. Sperber, T. Li, G. A. Meehl, 2005: MJO in the NCAR CAM2 with the Tiedtke convective scheme. *J Climate*, 18:3007–3020. doi:10.1175/JCLI3458.1

Liu, X., and coauthors, 2016: MJO prediction using the sub-seasonal to seasonal forecast model of Beijing Climate Center. Clim Dyn. doi:10.1007/s00382-016-3264-7

Ma, J., Y. Zhu, D. Wobus and P. Wang, 2012: An Effective Configuration of Ensemble Size and Horizontal Resolution for the NCEP GEFS. Advance in Atmospheric Sciences, Vol. 29, No. 4, 782-794

DRAFT

Maloney, E. D. and D. L. Hartmann, 2001a: The sensitivity of intraseasonal variability in the NCAR CCM3 to changes in convective parameterization. *J. Climate,* 14, 2015–2034.

Palmer, T., N., R. Buizza, F. Doblas-Reyes, T. Jung, M. Leutbecher, G. Shutts, M. Steinheimer, and A. Weisheimer, 2009: Stochastic parametrization and model uncertainty. Tech. Rep. ECMWF RD Tech. Memo. 598, 42 pp. [Available online at http://www.ecmwf.int/publications/.]

Pan, H. L. and W.-S. Wu, 1995: Implementing a mass flux convection parameterization package for the nmc medium-range forecast model. *NMC Office Note, No. 409*, page 40pp.

Pegion, K., and Sardeshmukh P.D., 2011: Prospects for improving subseasonal predictions. *Mon. Wea. Rev.* 139:3648–3666

Shutts, G., and T. N. Palmer, 2004: The use of high-resolution numerical simulations of tropical circulation to calibrate stochastic physics schemes. Proc. ECMWF/CLIVAR Simulation and Prediction of Intra-Seasonal Variability with Emphasis on the MJO, Reading, United Kingdom, European Centre for Medium-Range Weather Forecasts, 83 – 102.

Shutts, G. 2005: A kinetic energy backscatter algorithm for use in ensemble prediction systems. Q. J. R. Meteorol. Soc. 131, pp. 3079–3102

DRAFT

Tompkins, A. M., and J. Berner, 2008: A stochastic convective approach to account for model uncertainty due to unresolved humidity variability, J. Geophys. Res., 113, D18101.

Tracton, M. S., and E. Kalnay, 1993: Operational ensemble prediction at the National Meteorological Center: Practical aspects. Wea. Forecasting, 8, 379–398.

Tian, D. W., Eric and X. Yuan, 2017: CFSv2-based sub-seasonal precipitation and temperature forecast skill over the contiguous United States. Hydrol. Earth Syst. Sci., 21, 1477–1490.

Troccoli, A.: Seasonal climate forecasting, 2010: Meteorol. Appl., 17, 251–268, doi:10.1002/met.184.

Vitart, F., 2009: Impact of the Madden Julian oscillation on tropical storms and risk of landfall in the ECMWF forecast system. *Geophys. Res. Lett*., 36, L15802, doi:10.1029/2009GL039089.

Vitart, F., and F. Molteni, 2010: Simulation of the Madden–Julian Oscillation and its teleconnections in the ECMWF forecast system. *Quart. J. Roy. Meteor. Soc.*, 136, 842–855.

DRAFT

Vitart, F., 2014: Evolution of ECMWF sub-seasonal forecast skill scores. *Quart. J. Roy. Meteor. Soc*., 140, 1889–1899, doi:https://doi.org/10.1002/qj.2256.

Waliser, D.E., K.M. Lau, W. Stern, C. Jones, 2003: Potential predictability of the Madden–Julian oscillation. *Bull Am Meteorol Soc* 84:33–50

Wang, W., A. Kumar, J. X. Fu, and M.-P. Hung, 2015: What is the role of the sea surface temperature uncertainty in the prediction of tropical convection associated with the MJO? *Mon. Wea. Rev.*, 143, 3156–3175, doi:10.1175/MWR-D-14-00385.1.

Wang, W., and M. E. Schlesinger, 1999: The dependence on convection parameterization of the tropical intraseasonal oscillation simulated by the UIUC 11-layer atmospheric GCM. *J. Climate*, 12, 1423–1457.Wheeler, M.C and H. H. Hendon, 2004: An all-season real-time multivariate MJO index: Development of an index for monitoring and prediction. *Mon. Weather Rev.* 132*:* 1917–1932.

Zhang, G. J., and X. Song, 2009: Interaction of deep and shallow convection is key to Madden–Julian oscillation simulation. *Geophys. Res. Lett*., 36, L09708, doi:10.1029/2009GL037340.

DRAFT

Zhou, L., R. Neale, M. Jochum, and R. Murtugudde, 2012: Improved Madden–Julian oscillations with improved physics: The impact of modified convection parameterizations. *J. Climate*, 25, 1116–1136.

Zhou, X., Y. Zhu, D. Hou, Y. Luo, J. Peng, and R. Wobus, 2017: Performance of the New NCEP Global Ensemble Forecast System in a Parallel Experiment. Wea. Forecasting, 2017, https://doi.org/10.1175/WAF-D-17-0023.1

Zhu, Y., X. Zhou, M. Peña, W. Li, C. Melhauser, and D. Hou, 2017a: Impact of sea surface temperature forcing on Weeks 3 & 4 forecast skill in the NCEP Global Ensemble Forecasting System. *Weather and Forecasting*, 32, 2159–2174.

Zhu, Y., X. Zhou, W. Li, D. Hou, C. Melhauser, E. Sinsky, M. Peña, B. Fu, H. Guan, W. Kolczynski and V. Tallapragadaand, 2017b: An assessment of subseasonal forecast skill using an extended Global Ensemble Forecast System (GEFS), *J. Climate.* Submitted.

DRAFT

Table 1. Summary of the GEFS configurations

Abbreviation	**Stochastic Physics Scheme**	**SST**	**Convection Scheme**
STTP	STTP	Relax to Climatology.	SAS
SPs	SPPT+SHUM+SKEB	Relax to Climatology	SAS
SPs+CFSBC	SPPT+SHUM+SKEB	Initial analysis+ bias corrected CFS forecast	SAS
SPS+CFSBC+CNV	SPPT+SHUM+SKEB	Initial analysis+ Bias corrected CFS forecast	Updated SAS

DRAFT

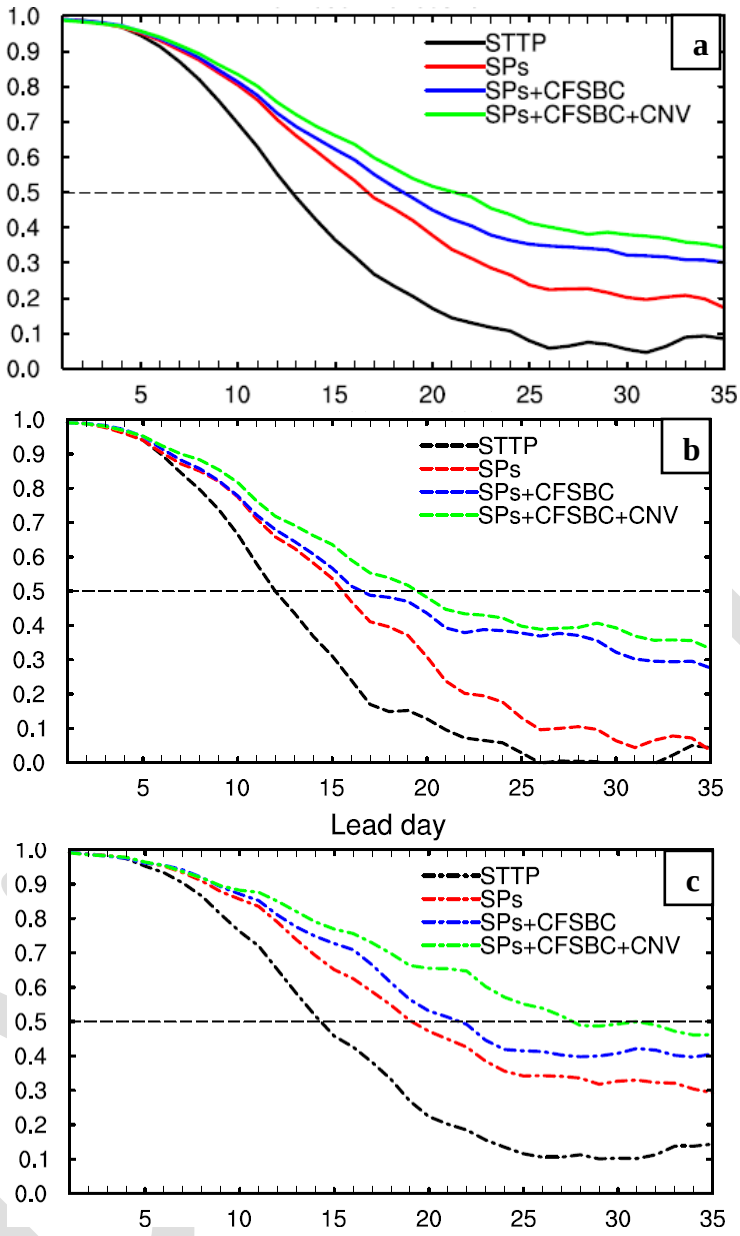

Figure 1. WH MJO skill for a). RMM1&2. b). RMM1. c). RMM2 for different experiments during the period of May 1st 2014-May 26, 2016 (5day-inteval). The WH-MJO skill is defined as the bivariate correlation between ensemble mean forecast and analysis data. Climatology and 120-day running mean are removed from the forecast and analysis data when calculating the RMMs. A dash line of anomaly correlation equals to 0.5 is added in the plot to indicate the MJO skill.

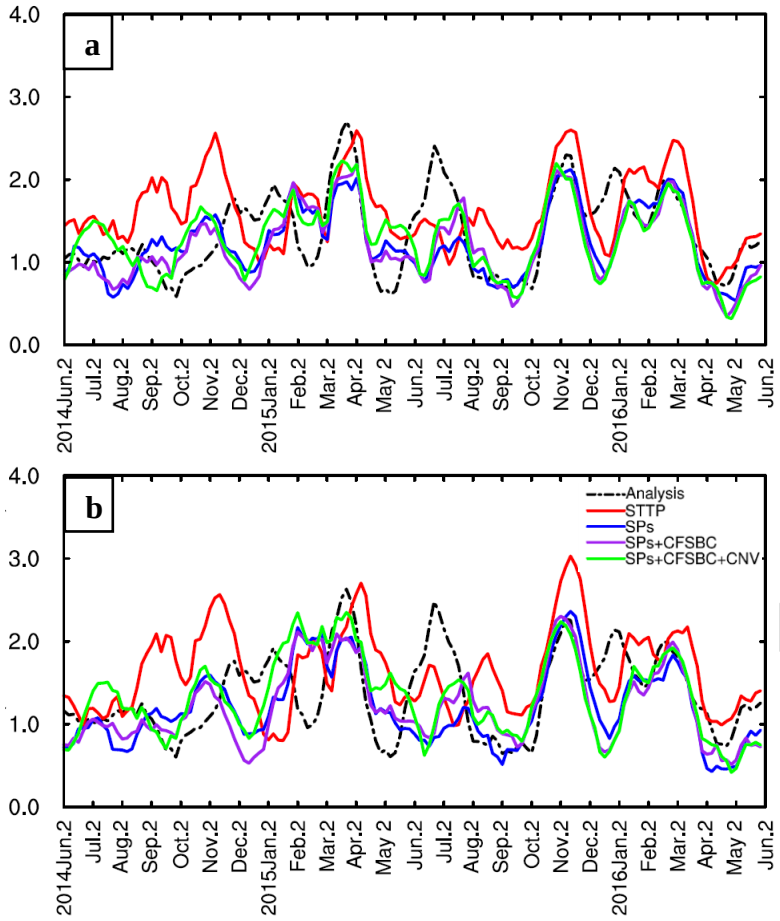

Figure 2. WH MJO index as a function of validation time for a). lead day=16 and b) lead day=21. 7 point running mean has been applied to the time-series to smooth the data.

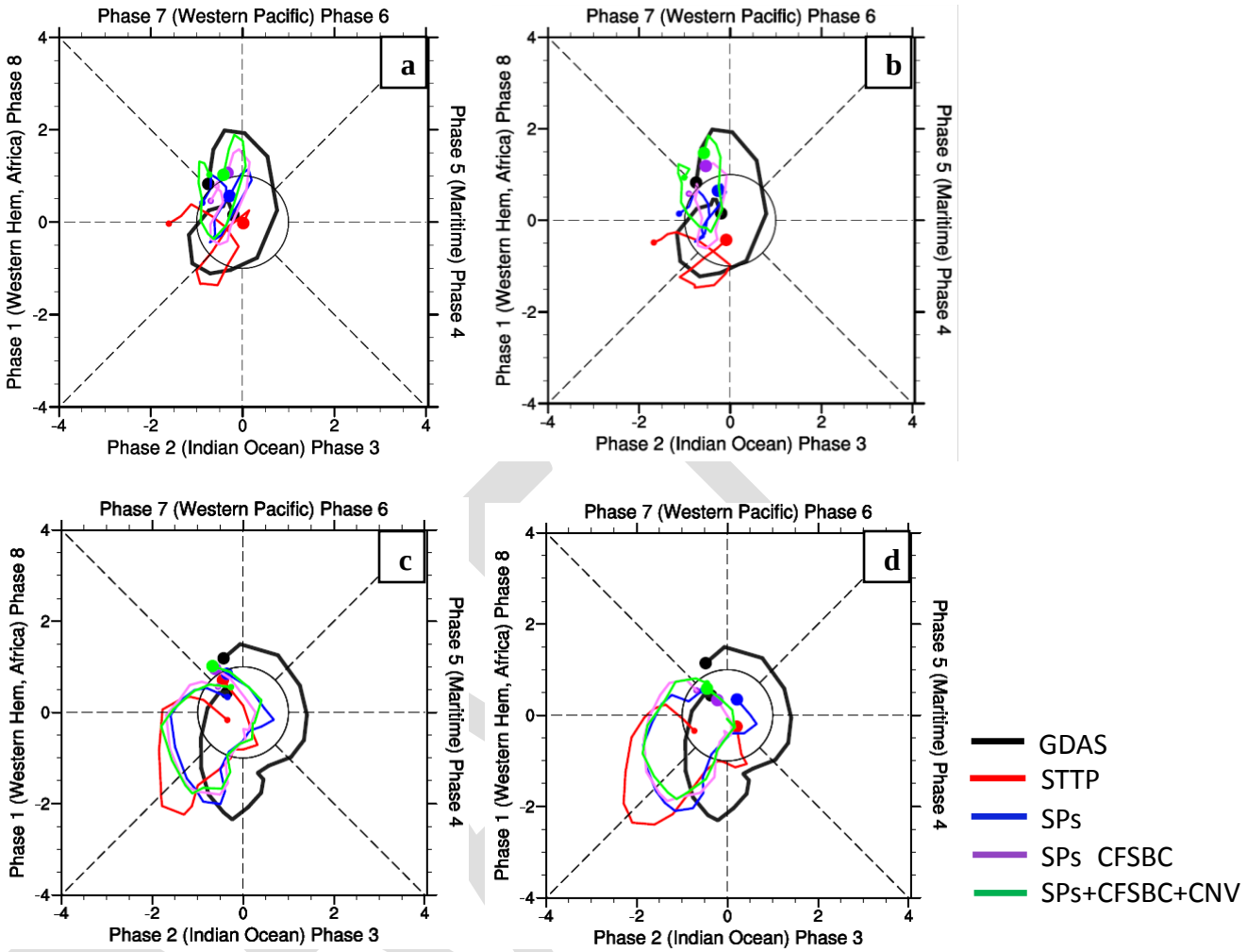

Figure 3. Phase diagram of the MJO index for lead day 16 (a and c) and 21 (b and d) during validation time of 20150502-20150717 (a and b) and 20151002-20160107 (c and d).

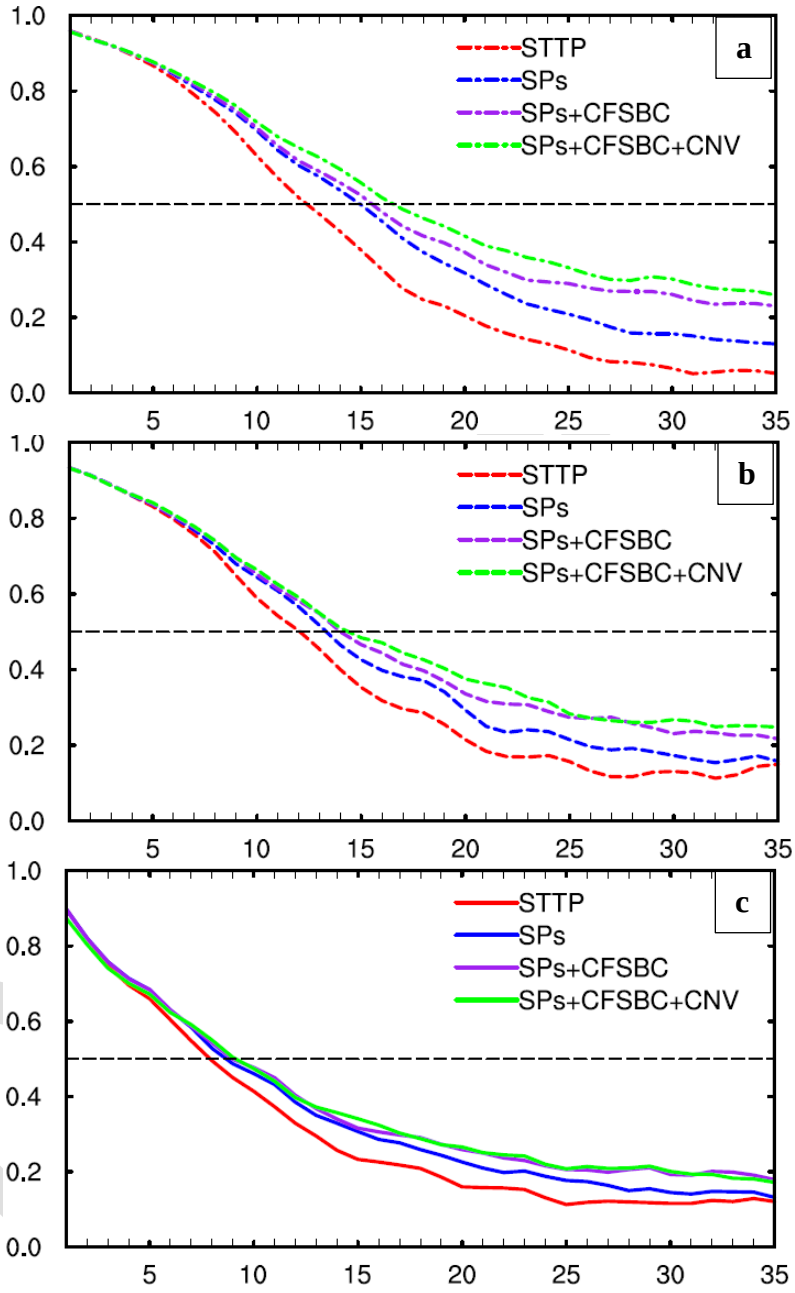

Figure 4. Correlation coefficient of a). U200; b) u850 and c). OLR anomalies over 15°S-15°N between the analysis and forecast data over the period of May 1st 2014-May 26 2016.

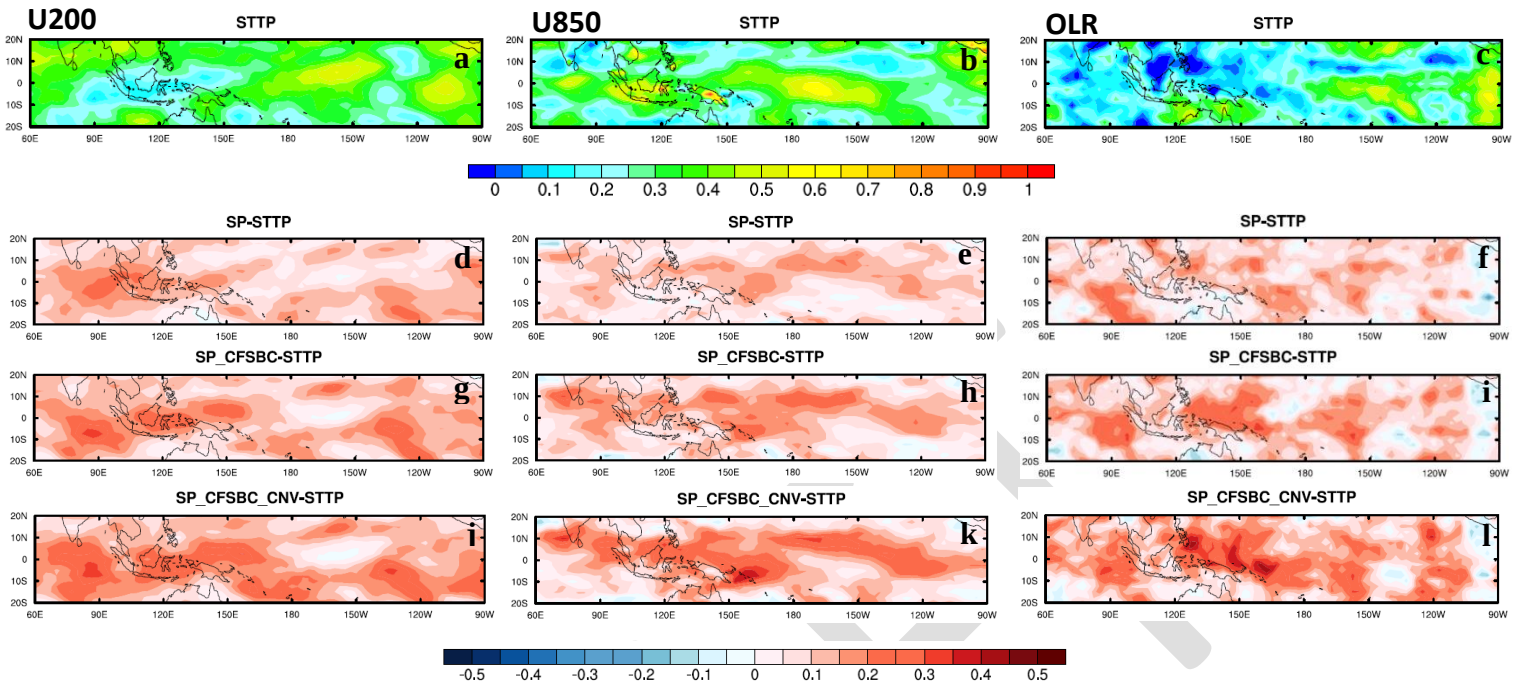

Figure 5. Spatial distribution of the correlation coefficient of u200, U850 and OLR anomaly between the analysis and the forecast data over the 2-year experiment period at lead day 15. a-c: Correlation coefficient for STTP; d-l: the difference of the correlation between the SPs experiments and the STTP.

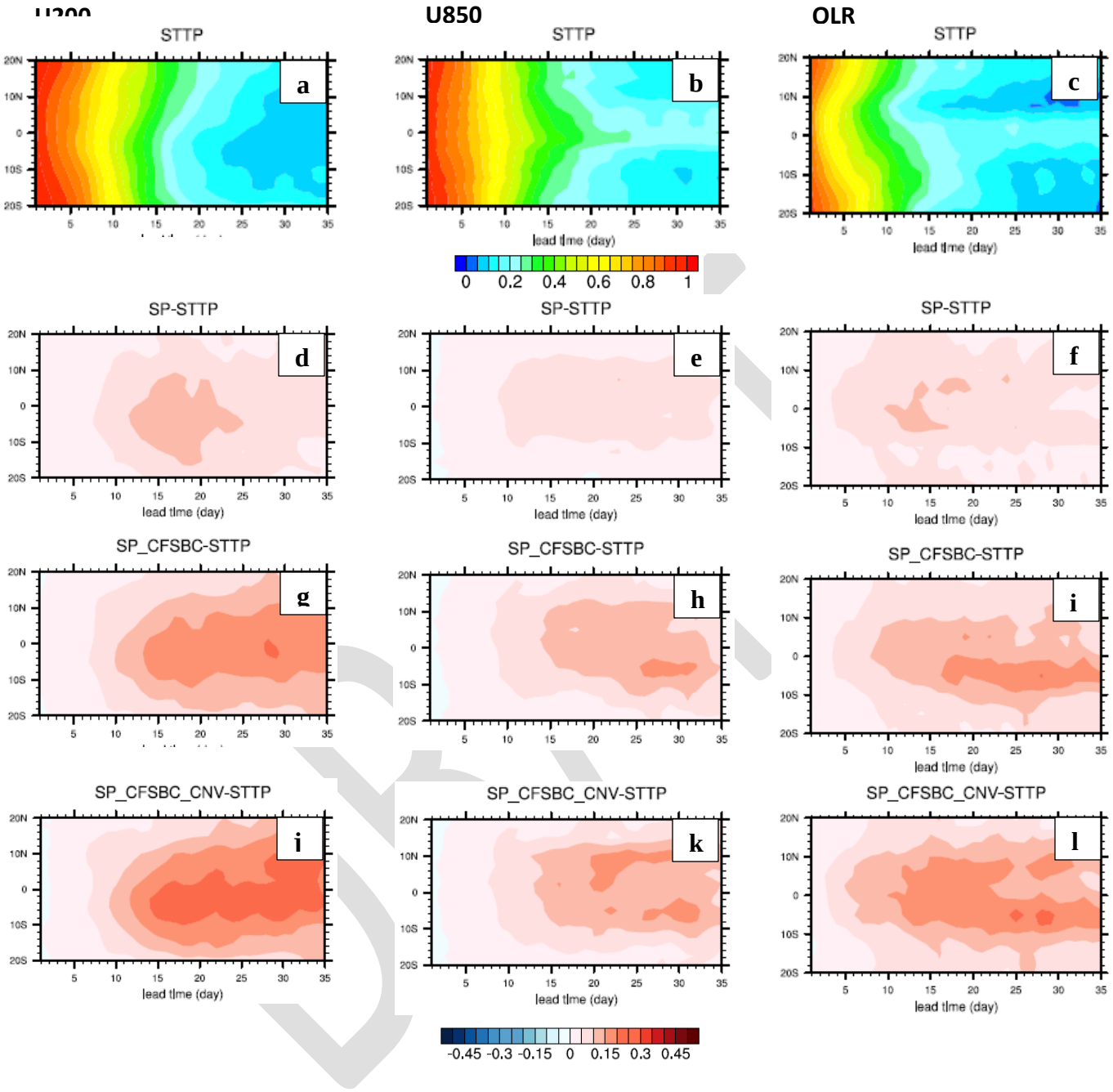

Figure 6. Correlation coefficient as a function of latitude and lead time for U200, U850 and OLR anomaly for STTP and the difference of the correlation coefficient of each experiment from the STTP.

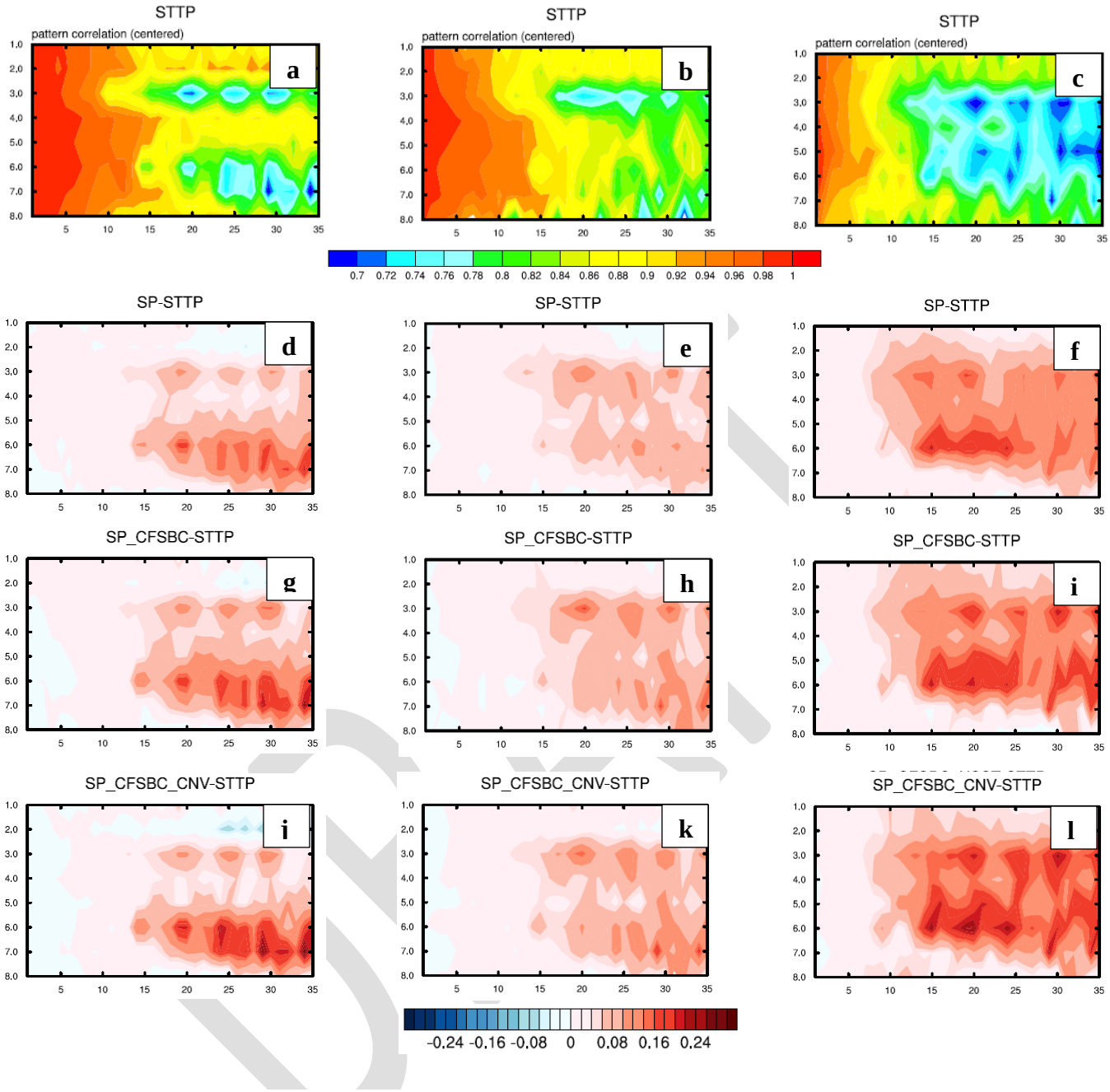

Figure 7. Pattern correlation as a function of MJO phase and lead time for the composite U200, U850 and OLR over each MJO phase between the analysis and forecast data. Left column: Pattern correlation for each experiment. Right column: difference of the pattern correlation between the SPs experiment and the STTP.

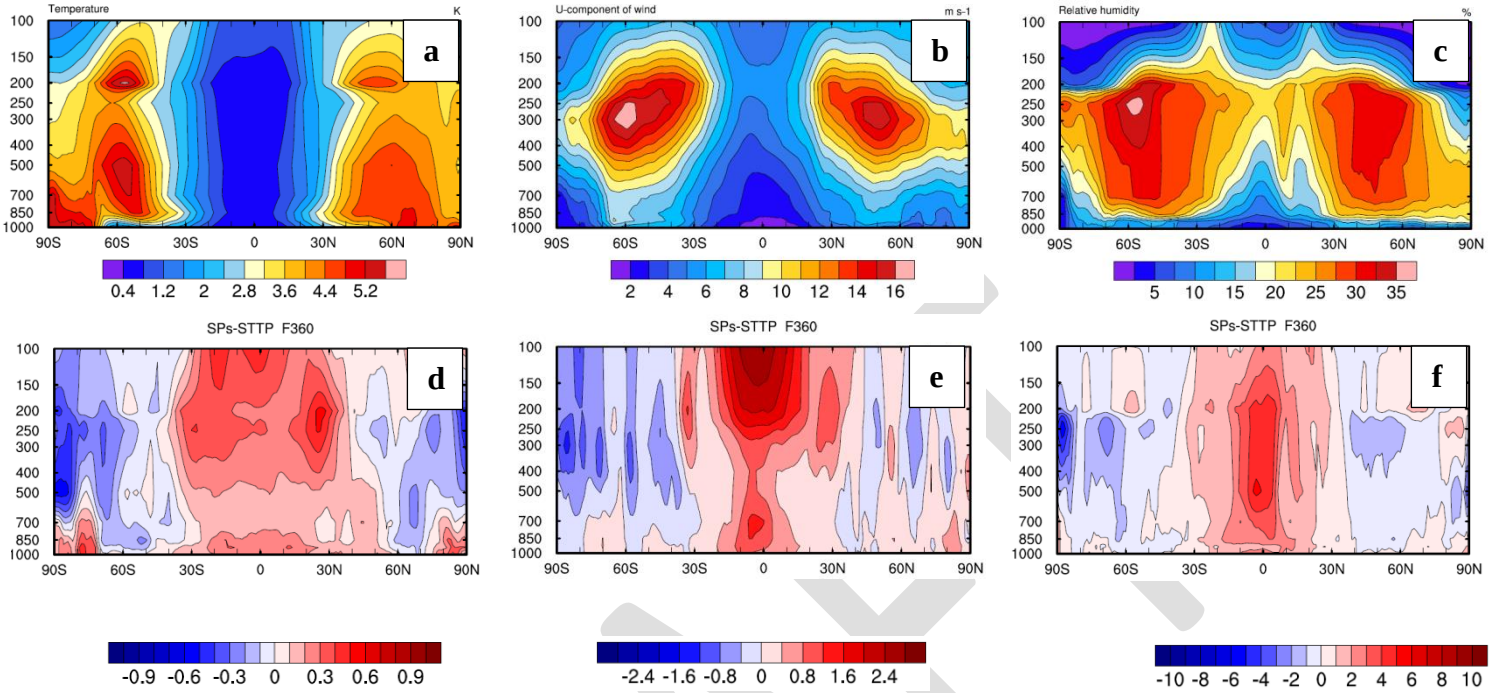

Figure 8. Ensemble spread of the perturbed members in GEFS for temperature (a), zonal wind (b) and relative humidity at 360th forecast hour (c) and the difference between SPs and STTP for the corresponding variables (d-f).

Draft

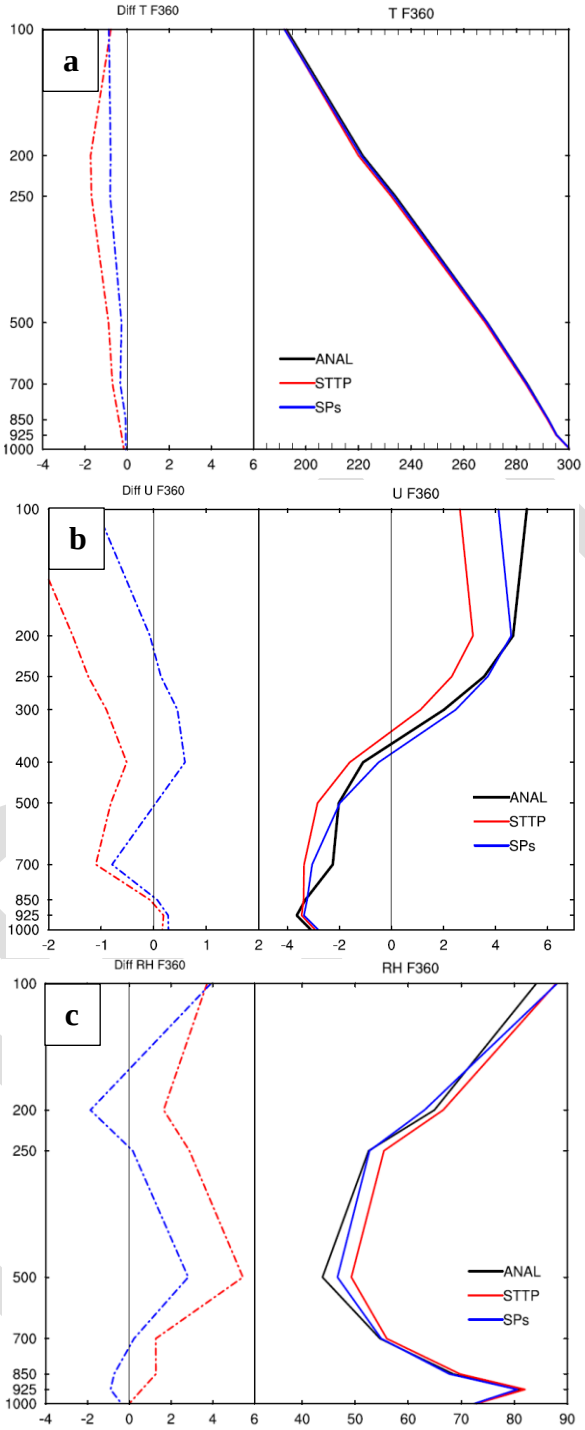

Figure 9. The 360-hour forecast of the temperature, zonal wind and relative humidity in Analysis, STTP and SPs (right panel of each plot) and the difference between each experiment and the analysis (left panel of each plot).

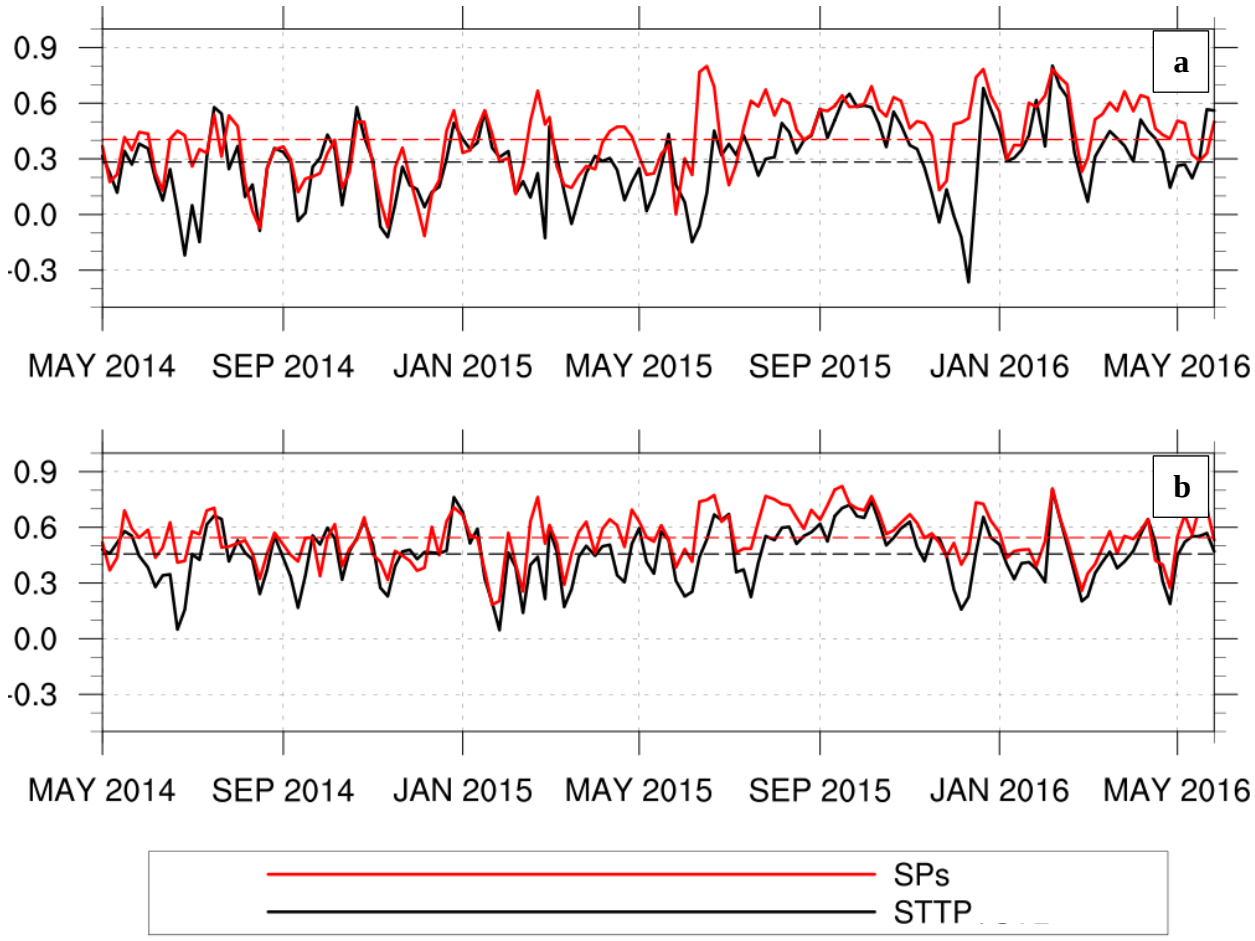

Figure 10. The ensemble mean anomaly correlation of the week 3&4 averaged 250 hPa (a) and 850 hPa (b) zonal winds as a function of initial time for the STTP and SPs. The average score for 250 hPa zonal wind (a) is 0.404 and 0.283 for SPs and STTP. The average score for 850 hPa zonal wind (b) is 0.545 and 0.457 for SPs and STTP respectively.